Steric interaction model of roughening and vacancy reorganization on halogen-terminated Si(100)-2×1 surfaces

Dongxue Chen and John J. Boland*
Venable and Kenan Laboratories, Department of Chemistry, University of North Carolina at Chapel Hill, Chapel Hill, North Carolina 27599-3290

(Received 23 September 2002; revised manuscript received 31 January 2003; published 27 May 2003)

We present a steric interaction (SI) model that describes roughening and reorganization on halogen-terminated Si(100)-2×1 surfaces. This model is based on parameters derived from density-functional theory total-energy calculations. Using these parameters together with the requirements for rebonding and atom conservation, it is possible to explain the types of reorganization events that can occur and the different steady-state morphologies observed in the presence of different halogen terminations. Using scanning-tunneling microscopy we show that dimer vacancy (DV) string elongation can occur by a process called primary roughening, i.e., the removal of pairs of dimers from the terrace and the formation/elongation of terrace islands. We show that experimentally and within the confines of the SI model end-on coalescence of DV strings is unfavorable but side-on coalescence can result in the formation of wider vacancy pits. In this manner the SI model explains why elongated vacancy pits are formed in the case of Br termination, whereas short, wider structures are observed with Cl. The model is also used to explain the nucleation of terrace islands and the attachment of dimers at islands and surface steps. The model predicts larger numbers of islands and enhanced roughness at S_B-type steps on the Br surface, in excellent agreement with experiment.

DOI: 10.1103/PhysRevB.67.195328 PACS number(s): 81.65.Cf, 68.37.Ef, 81.65.Rv

I. INTRODUCTION

The reaction of halogens with the Si(100) surface has been the subject of extensive research. Much of this interest stems from the crucial role of halogens in silicon chemical etching.[1] Etching has been shown to produce a range of surface morphologies that are dependent both on the etching temperature and the halogen used. Early studies attempted to explain these structures based on the relative rates of etching both along and perpendicular to the dimer row directions.[2] However, in a more recent study we showed that many of these morphologies are not due to etching but result from a thermodynamically favored roughing transition that is accessible at higher temperatures.[3] These results were confirmed by density-functional theory (DFT) calculations, which showed that the transition is driven by a reduction in steric interactions on the roughened surface.[3] However, the original study was restricted to the formation of simple vacancy strings and islands. Here in the present work we expand on this earlier study and demonstrate that the steric interaction (SI) model can be used to estimate the relative energies of arbitrary structures on the surface. We also suggest a multistep vacancy reorganization pathway based on our observations and show how steric interactions affect reorganizations by controlling the stability of intermediate structures. We present and compare static and real-time scanning-tunneling microscopy (STM) images of Br- and Cl-terminated Si(100) surfaces at elevated temperatures and show that the observed structures of the two systems are in excellent agreement with the SI model.

II. EXPERIMENT

All experiments were performed in a UHV STM system with a base pressure of 5×10^{-11} mbar. The samples used in this study were prepared by annealing 0.3-1.0 Ω cm phosphorous-doped Si(100) substrates to 1400 K to remove the native oxide. The clean surface was then heated and exposed to doses of 5.4×10^4 μA s of Br_2 or Cl_2 (approximately 1000 L) using an electrochemical cell.[4] All exposures were performed with the sample held at 600 K. Temperatures reported here are based on power-temperature calibration curves and are believed accurate to ±30 K. The overall halogen coverage was determined by calculating the concentration of the dangling-bond sites, which appear as bright spots in STM images and are easily identifiable. The surfaces shown were all near full coverage ($\theta>99.5\%$), which suggest that desorption of silicon halides is slow or negligible at the temperature reported here.

To study the equilibrium surface morphology, the surface was kept at the desired temperature for a certain period of time to allow equilibrium, then quenched and imaged at room temperature (see figure captions for details). Typically, a negative tip bias of −1.7 V was used to obtain empty-state images. Real-time imaging was also used to study the surface reorganization at high temperature. After preparation the surface was cooled to room temperature and subsequently heated on the STM stage to 300–1000 K while imaging. Surfaces were held at the same temperature for several hours, so that recorded events were either repetitive (e.g., site hopping) or occurred on time scales that were slow compared to our imaging speed (typically 100 nm/sec).

III. STERIC INTERACTION MODEL

It has been shown that under high-temperature conditions and in the absence of halogen gas, halogen-terminated surfaces are prone to spontaneous roughening.[3,5] Roughening occurs in two general forms. Primary roughening involves the removal of dimers strings from the surface to form dimer

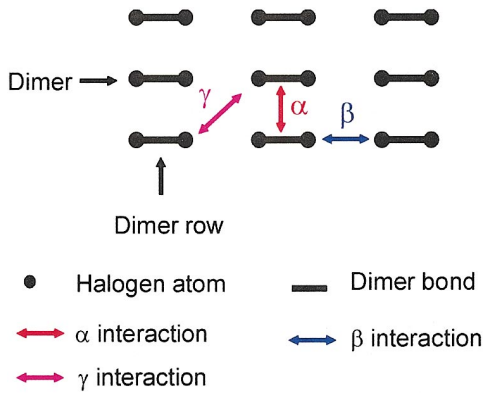

FIG. 1. (Color) Ball and stick model showing the steric repulsions on the full halogenated-Si(100)-2×1 surfaces. Only the silicon dimers and halogen atoms are shown. The steric repulsions between halogen atoms are represented by arrows, where α represents the intrarow repulsion and β represents the interrow steric repulsions. The secondary nearest-neighbor repulsion γ is also shown. However, as described previously (Ref. 3), γ repulsions are small and always cancels out. In our model, dimers are always fully halogenated, thus repulsions within the same dimer unit are not included.

vacancy (DV) strings and islands on the terrace.[3] In a secondary roughening step, these DV strings can dissociate into two single vacancy (SV) strings that are separated by *n* dimer units to produce regions with local $(2n+1)\times 2$ structures.[3,6,7] In each case, roughening breaks up the steric interactions present on the perfect terrace and allows local relaxation of the silicon-halogen bonds.[6,7] In this work we show how steric interactions play a pivotal role in determining the equilibrium morphologies that are ultimately observed on halogen-terminated Si(100) surfaces.

Steric interaction on the Si(100) surface can be parsed into two fundamental terms, α and β, which are shown schematically in Fig. 1. α steric interactions exist between pairs of halogen atoms in adjacent dimers of the same row. β interactions describe repulsions between nearest-neighbor halogen atoms in adjacent rows. Second-nearest-neighbor interactions (γ), although present, were previously shown to be negligibly small (~5 meV) for all halogens and do not make a significant contribution to the total energy.[3] The α and β repulsion energies calculated previously are shown for F, Cl, and Br in Table I. As expected, these repulsion energies scale with the size of the halogen atom. Previously we showed that with these repulsion energies and the known S_A and S_B step energies it is possible to describe the formation energies associated with primary and secondary roughening[3] by summing up the energy contributions from all components.[8] S_A and S_B step energies of 50 and 140 meV per 7.68 Å are assumed based on experimental and theoretical literature values.[9] Below, we expand on this analysis and show how these methods may be used to estimate the energy of arbitrary structures observed on Si(100) surfaces. Before proceeding we identify some salient aspects of the structure that play a key role in determining the types of surface structures and rearrangements that are permissible on the Si(100) surface.

TABLE I. Step energies and steric repulsion energies between halogen atoms on Si(100)-2×1 surfaces (Ref. 3). S_A and S_B step energies are 50 and 140 meV per 7.68 Å, respectively (Ref. 9).

	Intrarow α (meV)	Interrow β
Bromine	106	52
Chlorine	61	26
Fluorine	24	14

IV. SURFACE REBONDING AND ITS IMPLICATIONS

Steps and defects on halogen-terminated Si(100) surfaces are rebonded and this has important consequences for the types of vacancies and islands that can exist on this surface. The presence of rebonding is immediately evident from the fact that kinks at S_B steps are always two-dimer units in length. Because rebonding occurs almost everywhere the number of halogen and Si atoms is the same on both smooth and roughened surfaces,[3] and thus conservation of halogen atoms is an important consideration in all surface processes that involve pure rearrangements, i.e., roughening and vacancy reorganization.

Surface rebonding also gives rise to certain rules that govern the formation and elongation of DV strings and islands. To maintain the rebonded structure DV strings and islands must have lengths that correspond to an odd number of dimers. In addition, elongation and contraction events should occur in two-dimer units. These rules are consistent with our earlier experimental observations of the structure and dynamics of roughened halogen-terminated Si(100)-2×1 surfaces.[3] More importantly, since rebonding is conserved, regardless of the vacancy shape, the steric interactions involved are still well described by the α and β parameters of the SI model.

V. RESULTS AND DISCUSSION

To test the SI model we have studied the equilibrium morphologies of vacancies and islands on the Cl- and Br-terminated Si(100)-2×1 surfaces at elevated temperatures. Figure 2 shows representative room-temperature images following 2-h annealing up to temperatures around 850 K. For comparison purposes identical preparation procedures were used for both Cl- and Br-terminated surfaces (details are provided in the respective figure captions). Even casual inspection of the images in Fig. 2 reveals several important differences. The most striking difference is the asymmetry of the DV strings. In the case of Br there is a pronounced preference for single-dimer-wide DV strings. For Cl, these vacancies are often several-dimers wide and tend to have shapes approaching that of a square or a rectangle. This is further supported by our detailed analysis, which shows that the average pits widths are 1.04 ± 0.05 for the Br-terminated surface and 2.51 ± 0.35 for Cl. The average lengths of pits, on the other hand, are about the same for both Br and Cl, 7.95

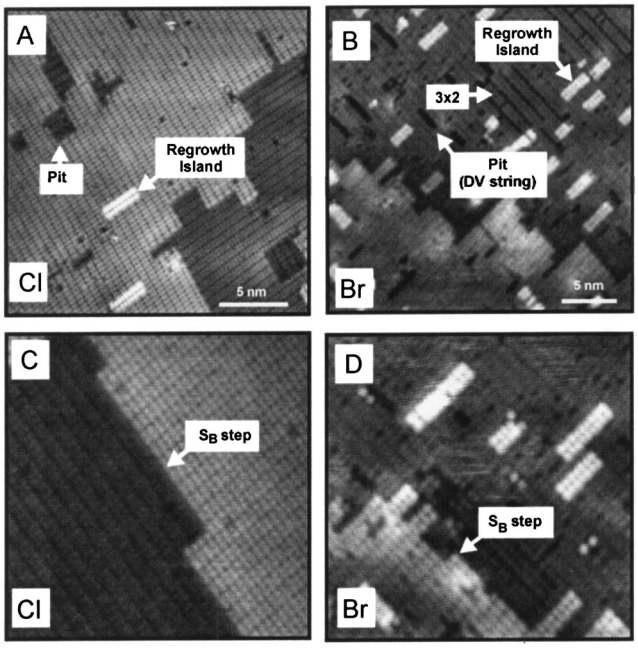

FIG. 2. Comparison of different equilibrium morphologies observed on Cl- and Br-terminated Si(100)-2×1 surfaces following 2-h annealing at 850 K. Bare surfaces were exposed to ~1000 L of halogen while held at 600 K. The surfaces were cooled down and imaged at room temperature to characterize the initial surface before annealing, which had little islands or pits (not shown here). Then the surfaces were heated up, kept at 850 K for 2 h, and quenched. Empty-state images, with a typical −1.7-V tip bias, were taken at room temperature. The surface coverage is initially ~100% and doesn't change significantly during the experiment (final coverage >99.5%). (a) Cl-terminated surface; major surface vacancies include both single- and multirow pits and regrowth islands. (b) Br-terminated surface; note that the pits are dominantly single-row DV strings; island density is higher compared with that of Cl-terminated surface. This surface also has some 3×2 features, which result from secondary roughening (see text). (c) Typical S_B steps of Cl-terminated surface. Note the step is smooth, with few kinks. (d) Typical S_B steps of Br-terminated surface. Steps are rougher compared with those of the Cl surface. More peninsulas are present along S_B steps.

±1.84 and 7.51 ± 1.44, respectively. Here, width and length are defined as the number of dimer units in the dimer bond direction and dimer row direction, respectively.

Another notable difference is the number of islands; there are many more islands on the Br-terminated surface for which the islands-to-pits area ratio is 0.87 ± 0.08. For the Cl surface, this ratio is 0.37 ± 0.16. Also, on the Cl-terminated surface we frequently observe multiple row islands, which are absent on the Br surface.

Finally, step shapes are also different for Br- and Cl-terminated surfaces. Figures 2(c) and 2(d) show that S_B steps are typically rougher for Br surfaces, and tend to be comprised of long peninsular structures while those on Cl surfaces are much smoother. Below, we detail how the SI model is able to explain the halogen dependence of the Si(100) surface morphology.

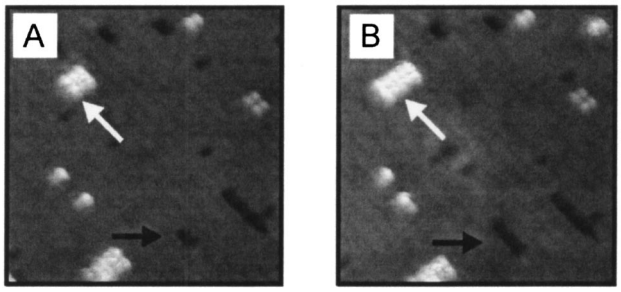

FIG. 3. Consecutive empty-state STM images of Si(100)-2×1:Br recorded at 800 K. Image size ~13 nm^2; tip bias −1.7 V. The 3-DV string in (a) extends by two dimer units into a 5-DV string in (b) (white arrow); at the same time, a three-dimer island elongates into a five-dimer island (black arrow). Both silicon and halogen atoms are conserved during this process.

A. DV string nucleation and elongation

DV string formation is a key aspect of primary roughening and allows the halogen atoms on the dimer rows on either side of the string to relax into the vacancy.[3] DV string nucleation requires the presence of single isolated DV's (1-DV's), which are known to have a rebonded structure.[10] 1-DV's are commonly found on Si(100) surfaces, and at high temperatures, are readily created at steps. Once a 1-DV exists it can be readily extended by primary roughening. To comply with the rebonding rules, extensions must occur in two dimer units, thus guaranteeing that the string will remain odd in length. Figure 3 shows one such elongation event where the existing DV string is extended by popping out two dimer units. Within the SI model[3] the energy gained in this process is $+2S_A-a-2\beta$, where S_A is the Si(100) S_A step energy per unit length (7.68 Å).[7] Using Table I, we estimate that this energy is −110 meV for Br and −13 meV for Cl. The Si atoms liberated in this process append to an existing island (see Fig. 3), but they could, in principle, also attach at nearby steps or even occasionally fill another surface vacancy. The energy gained from step or island attachment is the same, i.e., $+2S_A-a-2\beta$. Thus in the case of primary roughening, half the energy gain comes from DV elongation, while the other half comes from dimer attachment at islands or steps. This symmetry reflects the fact that both vacancies and islands share a common rebonded structure.

Primary roughening is the dominant mechanism for DV string elongation because coalescence of existing DV strings in the same row is prohibited. This follows directly from the rebonding requirement that favors odd DV lengths. However, since long-length DV strings have large effective masses and hence reduced mobility, such processes would be rare even if allowed. Earlier we demonstrated that 1-DV's are mobile at temperatures above 750 K (Ref. 5) and so can be used to study end-on coalescence. Figure 4 provides direct evidence that coalescence of a 1-DV and a long-length DV string is unfavorable. This real-time sequence clearly shows a 3-DV string and 1-DV in Fig. 4(a) that combine to form an unfavorable 4-DV in Fig. 4(b) that subsequently dissociates again in Fig. 4(c). It is important to point out that these restrictions only apply to coalescence of DV strings in the same dimer row. Coalescence of DV strings from two neighboring rows

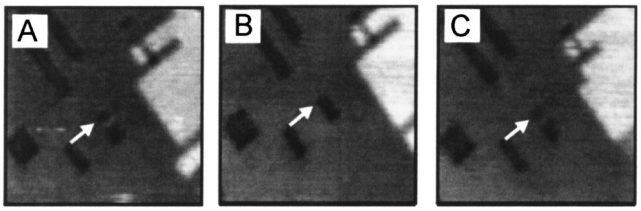

FIG. 4. Consecutive empty-state STM images of Si(100)-2 $\times$1:Cl recorded at 800 K. Image size ~9 nm^2; tip bias -1.7 V. This series shows that the end-on attachment of two DVs (strings) is higher in energy than two separate vacancies. (a) A 1-DV next to a 3-DV string in the same dimer row. (b) The 1-DV coalesces with the 3-DV to form a 4-DV string, which violates the rebonding rule, and thus is unstable. (c) The unstable 4-DV string dissociates back into 1-DV and 3-DV strings.

is possible and may actually play an important role in the formation of wider vacancy pits (see below).

In addition, atom conservation and rebonding arguments show that it is not possible for a one-dimer-wide DV string to change shape by pure vacancy rearrangement. Simple counting arguments show that the number of halogen atoms cannot be conserved in any rearrangement that involves an increase in the width of the DV string. For example, a rearrangement involving the formation of a two-dimer-wide string (n_1-DV:n_2-DV, where $n=n_1+n_2$) from a single-dimer-wide n-DV string violates both the rebonding rule (which requires odd length strings) and atom conservation. Rearrangements involving formation of a three-dimer-wide string are also prohibited, this time based solely on atom conservation.

Although widening of DV strings through pure rearrangement is not possible, the sideways coalescence of DV's provides a possible pathway for the formation of wider vacancy pits through pure rearrangement. The analysis provided below is valid, provided the rearrangement is a multistep process. In that case the energies of stable intermediate structures can be described by the SI model, subject to rebonding and atom conservation rules discussed earlier. Figure 5(a) schematically describes the side-on coalescence of a 1-DV with an existing DV string, and the energy difference within the context of the SI model is also shown. Following 1-DV attachment to an existing DV, the total S_A step length is shorter by one-unit length (7.68 Å), and there is one additional pair of β repulsions. Thus the total-energy change is $-S_A+\beta$, which is -24 meV for Cl and $+2$ meV for Br (see Table I). Thus for Cl, this attachment is favorable while for Br, it is somewhat disfavored and the entropy reduction associated with this process could prevent it from occurring in the latter case. When the 1-DV is lined up with one end of the existing DV string, the number of kinks is reduced by two and attachment becomes more favorable. This is consistent with the appearance of a large number of L-shaped vacancy pits, particularly on the Cl surface (see Fig. 6). Using similar counting methods, it is possible to show that sideways coalescence of two DV strings (i.e., longer than 1-DV) is not favored, with the associated energy being $-2S_A+a+2\beta$ per two dimer units (i.e., $+110$ meV for Br and $+13$ meV for Cl). These results show that 1-DV species are special. Although 1-DV's are rebonded and satisfy the counting rules, they are the only vacancy structures that do not contain halogen atoms. As a result they have unique combining properties that allow them to play a special role in the surface vacancy nucleation and rearrangement.

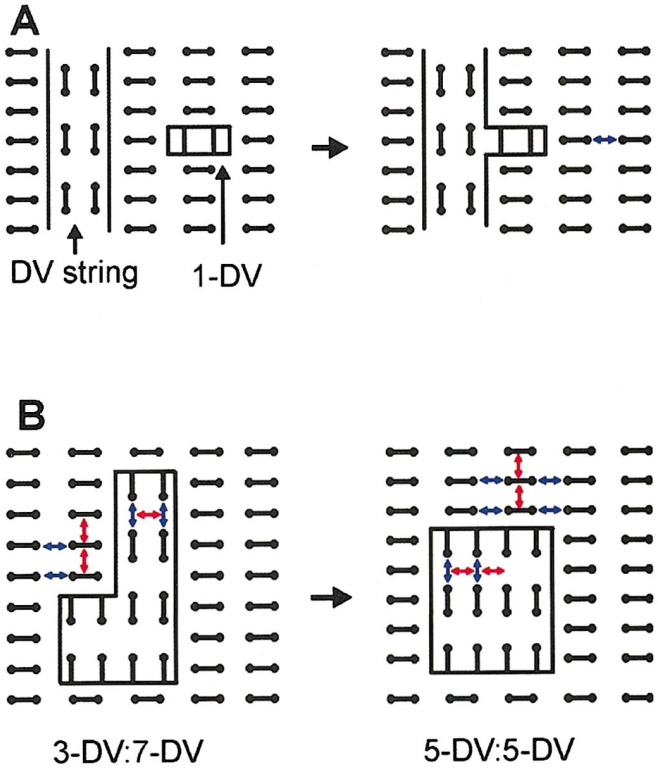

FIG. 5. (Color) Ball and stick model showing energies involved in certain surface rearrangements within the SI model. The left panel represents the surface before rearrangement, where the arrows identify the steric repulsions that will disappear after rearrangement. The color labeling follows the same scheme as Fig. 1. The right panel represents the final morphology and the arrows indicate the new steric repulsions that are created. The changes in step length are determined by straightforward counting and are omitted for simplicity. (a) Sideways attachment of a single DV to an existing DV string. The left panel shows the separated DV string and single DV while the right panel shows the coalesced vacancies. Note that total length of S_A steps drops by one unit length (7.68 Å), while one more pair of β repulsions exists on the surface (the arrow in right panel), thus the total-energy change during this process is $-S_A+\beta$. (b) Pure rearrangement of a 3-DV:7-DV pit into a 5-DV:5-DV pit. Such a rearrangement conserves atoms and also obeys the rebonding rules (see text). Simple counting shows that $2\alpha+2\beta$ from the upper terrace and $\alpha+2\beta$ from the lower terrace (in the pit) are removed, while $2\alpha+4\beta$ at upper terrace and $2\alpha+2\beta$ at the lower terrace are introduced after rearrangement. With the total S_A step it drops by two unit lengths (2×7.68 Å), and the total-energy gain is $-2S_A-(2\alpha+2\beta)-(\alpha+2\beta)+(2\alpha+4\beta)+(2\alpha+2\beta)$ or $-2S_A+\alpha+2\beta$.

After a two-dimer-wide vacancy pit is formed by side-on attachment of a 1-DV, both the longer and shorter branches can elongate by primary roughening. For the longer branch, the energy of primary roughening is the same as that for a normal one-row-wide DV string. However, for the shorter

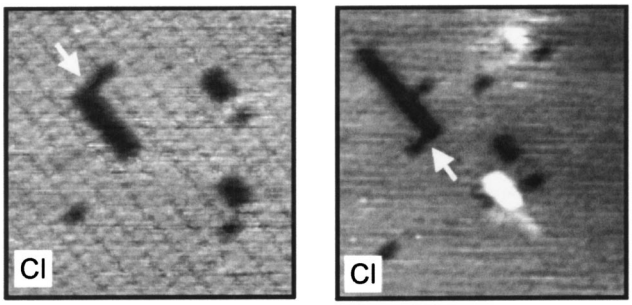

FIG. 6. Empty-state STM images of Si(100)-2×1:Cl surface recorded at 800 K. The L-shaped pit consists of a long DV string and a single DV that is lined up with one end of the DV string. Attachment at the end (to form an L-shaped vacancy) is favored because of a reduced number of kinks.

branch, there is no energy gain directly by removing additional dimers, because the step lengths and halogen repulsions remain unchanged. The total energy, however, is still lowered in the latter process since the dimers liberated by DV elongation can attach at nearby islands or steps. Thus, the primary roughening energy for sites along the shorter branch is only half that associated with a normal one-dimer-wide DV string.

For wider vacancy pits, it is permissible to rearrange the vacancies as long as the width does not change and all strings remain odd in length. For example, an 11-DV:3-DV structure can rearrange to form a 9-DV:5-DV or a 7-DV:7-DV structure. To estimate the energies involved in such rearrangements, we present an analysis of a 7-DV:3-DV structure converting to a 5-DV:5-DV structure. Figure 5(b) shows that after the rearrangement, the total S_A step length is shorter by two-unit lengths (2×7.68 Å), and repulsions increase by a on the lower terrace and 2β on the upper terrace, so the total energy involved is $-2S_A+a+2\beta$ (per two dimer units). This process is very unfavorable for Br (+110 meV), but much less so for Cl (+13 meV). Within the SI model, kink sites are not explicitly considered. However, whenever the rearrangement results in the formation of a symmetric square or rectangular pit (e.g., 5-DV:5-DV) the energy will actually be lower since there is an added reduction associated with the elimination of the kink site associated with the original asymmetric vacancy.

In summary, within the confines of the SI model, primary roughening is the dominant mechanism of extending the length of DV strings. The SI model predicts that primary roughening favors Br over Cl, which is in agreement with experiment. Moreover, within the SI model the most important pathway for forming wider pits is the sideways coalescence of 1-DV to a second DV string. It is favorable on the Cl surface but not so on the Br surface. Once wider pits form, they can elongate through primary roughening. Thus, chlorinated surfaces should tend to have wider pits. Once these wider pits form they can subsequently rearrange into square or rectangular shapes more easily on the Cl surface compared to the Br surface, once again in agreement with the experimental observations in Fig. 2.

B. Island formation and attachment at steps

The formation of terrace islands is another key aspect of primary roughening. This allows the halogen atoms on the island to relax and avoid the inherent repulsions between neighboring dimer rows that make up the terrace itself. However, unlike DV strings, which are readily nucleated by existing 1-DV's, the silicon and halogen atoms produced by DV formation must nucleate to form terrace islands or attach at nearby steps.[11] Straightforward nucleation of a single-dimer island by removing a dimer from the terrace violates atom conservation rules. Here we suggest a mechanism for island nucleation that conserves atoms and obeys the rebond-

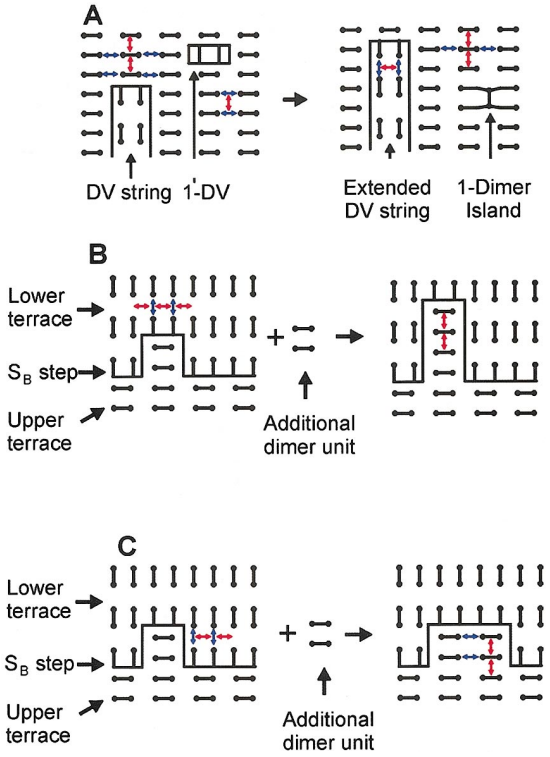

FIG. 7. (Color) Ball and stick model showing the energy involved in island nucleation (a) and when dimer units append to steps (b) and (c). Steric repulsions are labeled with the same color scheme as in Figs. 1 and 5. (a) Possible island nucleation mechanism. One of the two dimer units produced by extending a DV string (primary roughening) is absorbed into a nearby 1-DV while the other one binds to four top-layer Si atoms without breaking any dimer bonds. Careful counting shows that both halogen and silicon atoms are conserved. The energy changes are $2S_A+\alpha+2\beta-(2\alpha+4\beta)$ for extending the DV string, $-(S_A+2S_B)+2\alpha+2\beta$ from filling the 1-DV, and $S_A+2S_B-(\alpha+2\beta)$ from formation of the single-dimer island, which sums up to $2S_A-2\beta$. (b) Attachment of two dimer units to an existing peninsula, which results in the formation of a longer peninsula. The S_B step runs horizontally, with the upper terrace at the bottom and the lower terrace at the top. The two additional dimer units are produced by primary roughening, i.e., extending a nearby DV string. Using our counting scheme, it can readily be shown that the total-energy change is $2S_{A-a}-2\beta$. (c) Attachment of two dimer units to a S_B step next to an existing peninsula. Although this results in wider peninsulas and ultimately smoother S_B steps, the total-energy gain is zero.

ing rules. Consider an allowed roughening event that removes two dimer units from the terrace. Since a two-dimer island violates rebonding, we consider a scenario where one of the dimers fills a nearby 1-DV. The other dimer unit bonds to the four top-layer silicon atoms from two neighboring dimer rows without breaking any dimer bonds. The result is a strained single-dimer island but with the desired rebonded S_B steps on both sides [see Fig. 7(a)]. When additional dimer units (produced by primary roughening) attach, the island becomes stabilized.[11] Significantly, during this entire process, rebonding and atom conservation rules apply so we can use the SI model to estimate the relative energy for island nucleation on the Br and Cl surfaces. Island nucleation can be broken down into three parts: elongation of the DV string, filling of a 1-DV, and formation of the one-dimer island. Using the counting scheme discussed earlier, we can determine that the energies associated with DV elongation, filling of a single DV, and single-dimer island formation are $2S_A - a - 2\beta$, $-S_A - 2S_B + 2a + 2\beta$, and $S_A + 2S_B - a - 2\beta$, respectively [see Fig. 7(a)]. Together, the total energy of island nucleation is $2S_A - 2\beta$, i.e., -4 meV for Br and 48 meV for Cl. The enhanced entropy at higher temperature will further favor these processes. In any case, island nucleation is more costly for Cl than for Br and so, in agreement with experiment, the island density is predicted to be higher on the Br surface.

Following nucleation, the shape and distribution of islands on the surface can significantly influence the total surface energy. For instance, based on the definition of a and β, it is readily apparent that large interdimer β interaction favors long islands, whereas small β interaction favors wider multirow islands. On this basis alone one can predict that the Br surface will favor long single-row islands or more separated islands, whereas Cl surfaces tend to have some multirow islands, consistent with the STM results. Moreover, when the island density becomes large, island formation is no longer an efficient means to reduce steric repulsions. For example, when one-row-wide islands are grouped together to form wider multirow island, there is an increase in steric repulsions together with decreases in surface step energy. This in fact is the inverse of primary roughening. For this reason it is energetically favorable to pack islands as close together as possible without forming a continuous multirow island. The result is a 3×2 structure where each island is separated by a single missing row of atoms (i.e., an SV). This 3×2 structure is routinely observed on the Br surface at high temperatures[2,6] and is also observed on the terrace following secondary roughening.[3]

Instead of attaching at an existing island, dimers units may append to an existing step. When the dimer units attach to a flat S_B step or the end of a peninsula at an S_B step, the energy gain is the same as attaching to an existing island, i.e., $2S_A - a - 2\beta$ [-110 meV for Br and -13 meV for Cl, Fig. 7(b)]. But if the dimer units attach to an S_B step, next to a peninsula [see Fig. 7(c)], so as to yield a smoother S_B step, there will be no energy gain at all. Since attachment at the end of peninsulas is more favored for Br than for Cl (-110 vs -13 meV), this suggest that an S_B step on a Br-terminated surface should be much rougher than for Cl, in general agreement with the result in Figs. 2(c) and 2(d).

VI. CONCLUSIONS

We have presented a steric interaction (SI) model that describes roughening and vacancy reorganization on halogen-terminated Si(100)-2×1 surfaces. This model is based on parameters derived from DFT total-energy calculations. Using these parameters together with the requirements for rebonding and atom conservation, it is possible to explain the types of reorganization events that can occur and the different steady-state morphologies observed in the presence of different halogen terminations. The predictions of this model are in excellent agreement with our experimental STM results. Although in this present work we have used the SI model to describe the relative energy of specific surface structures, we are confident that it is capable of describing arbitrary structures on these surfaces. Moreover, extensions of this model may be applicable to other nonhalogen surface terminations.

*Author to whom correspondence should be addressed. Present address: Department of Chemistry, Trinity College, Dublin, Ireland. Email address: jboland@tcd.ie

[1] H. F. Winters and J. W. Coburn, Surf. Sci. Rep. **14**, 161 (1992).
[2] C. M. Aldao and J. H. Weaver, Prog. Surf. Sci. **68**, 189 (2001), and references therein.
[3] C. F. Herrmann, D. Chen, and J. J. Boland, Phys. Rev. Lett. **89**, 096102 (2002).
[4] N. D. Spencer, J. J. Goddard, P. W. Davies, M. Kitson, and R. M. Lambert, J. Vac. Sci. Technol. A **1**, 1554 (1983).
[5] K. S. Nakayama, C. M. Aldao, and J. H. Weaver, Phys. Rev. Lett. **88**, 125508 (2002).
[6] C. F. Herrmann and J. J. Boland, Phys. Rev. Lett. **87**, 115503 (2001).
[7] D. Chen and J. J. Boland, Surf. Sci. Lett. **518**, 583 (2002).
[8] D. Vanderbilt, Phys. Rev. B **36**, 6209 (1987).
[9] H. J. Zandvliet, Rev. Mod. Phys. **72**, 593 (2000), and references therein.
[10] J. H. G. Owen *et al.*, Surf. Sci. **341**, L1042 (1995).
[11] Y.-W. Mo, B. S. Swartzentruber, R. Kariotis, M. B. Webb, and M. G. Lagally, Phys. Rev. Lett. **63**, 2393 (1989).